JACS
JOURNAL OF THE AMERICAN CHEMICAL SOCIETY
Article
pubs.acs.org/JACS

Brightness Enhanced DNA FIT-Probes for Wash-Free RNA Imaging in Tissue

Felix Hövelmann,[†] Imre Gaspar,[‡] Anne Ephrussi,[‡] and Oliver Seitz*,[†]

[†]Institut für Chemie der Humboldt-Universität zu Berlin, 12489 Berlin, Germany
[‡]European Molecular Biology Laboratory, 69117 Heidelberg, Germany

Supporting Information

ABSTRACT: Fluorogenic oligonucleotides enable RNA imaging in cells and tissues. A high responsiveness of fluorescence is required when unbound probes cannot be washed away. Furthermore, emission should be bright in order to enable detection against autofluorescent background. The development of fluorescence-quenched hybridization probes has led to remarkable improvement of fluorescence responsiveness. Yet, comparably little attention has been paid to the brightness of smart probes. We describe hybridization probes that combine responsiveness with a high brightness of the measured signal. The method relies upon quencher-free DNA forced intercalation (FIT)-probes, in which two (or more) intercalator dyes of the thiazole orange (TO) family serve as nucleobase surrogates. Initial experiments on multi-TO-labeled probes led to improvements of responsiveness, but self-quenching limited their brightness. To enhance both brightness and responsiveness the highly responsive TO nucleoside was combined with the highly emissive oxazolopyridine analogue JO. Single-stranded TO/JO FIT-probes are dark. In the probe−target duplex, quenching caused by torsional twisting and dye−dye contact is prevented. The TO nucleoside appears to serve as a light collector that increases the extinction coefficient and transfers excitation energy to the JO emitter. This leads to very bright JO emission upon hybridization (F/F_0 = 23, brightness = 43 mL mol^{-1} cm^{-1} at λ_{ex} = 516 nm). TO/JO FIT-probes allowed the direct fluorescence microscopic imaging of *oskar* mRNA within a complex tissue. Of note, RNA imaging was feasible under wide-field excitation conditions. The described protocol enables rapid RNA imaging in tissue without the need for cutting-edge equipment, time-consuming washing, or signal amplification.

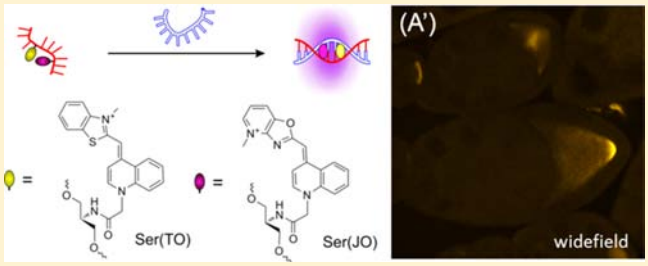

INTRODUCTION

Fluorescently labeled oligonucleotides are among the most important tools used to detect and localize specific nucleic acid targets in biological fluids, cells, and tissues.[1−4] Significant effort has been invested in the development of smart probes that show increases in fluorescence upon hybridization. Such responsive probes enable applications in real-time PCR,[5] fluorescent in situ hybridization (FISH), and live cell RNA imaging[6] when separation of unbound probes is undesired, difficult, or even impossible.

The performance of fluorogenic hybridization probes within cellular systems is characterized by two main features: responsiveness and brightness of fluorescent signaling. High responsiveness is required for discrimination of the unbound probe, whereas brightness is critical to reliably detect the probe signal against a given fluorescence background of the cell. The introduction of DNA-based molecular beacons marked an important event in nucleic acid technology.[7] In the original molecular beacon format, hairpin formation is used to bring two terminally appended dyes into proximity. Hybridization with the target opens the hairpin structure. The increase of the distance between the reporter fluorophore and the quencher dye is accompanied by enhancement of fluorescence emission. Substantial efforts have been focused on the development of enhanced molecular beacon type probes. Metals,[8] small molecules,[9] as well as modifications of the hairpin stem[10−13] influence fluorescence quenching in the unbound state and, therefore, allowed improvements of the achievable signal-to-background ratio. The use of enhanced quencher dyes,[14,15] nanoparticles,[16−19] or graphene[20−23] allowed further increases in fluorescence quenching. To foster dye−dye interactions, fluorescent dyes were incorporated as base surrogates within the double helical stem region[24−29] or coupled to peptide nucleic acid (PNA) scaffolds.[30,31] Recently, intracellular RNA was detected by means of target-triggered fluorogenic reactions between two reactive probes.[32,33]

The described efforts have led to remarkable improvement of the fluorescence responsiveness. However, comparably little attention has been paid to the brightness of fluorescent signaling. The quencher moieties typically involved inevitably reduce brightness, not only in the unbound state, but also in the target-bound state of the probe. For envisaged applications in wash-free FISH and live cell RNA imaging we sought hybridization probes that combine responsiveness with the

Received: October 24, 2013
Published: December 2, 2013

   dx.doi.org/10.1021/ja410674h | J. Am. Chem. Soc. 2013, 135, 19025−19032

high brightness of fluorescent signaling required to detect and localize mRNA in autofluorescent tissues.

Our work relies upon quencher-free DNA FIT-probes, in which an intercalator dye of the thiazole orange (TO) family serves as a surrogate nucleobase (Figure 1A).[34] Hybridization

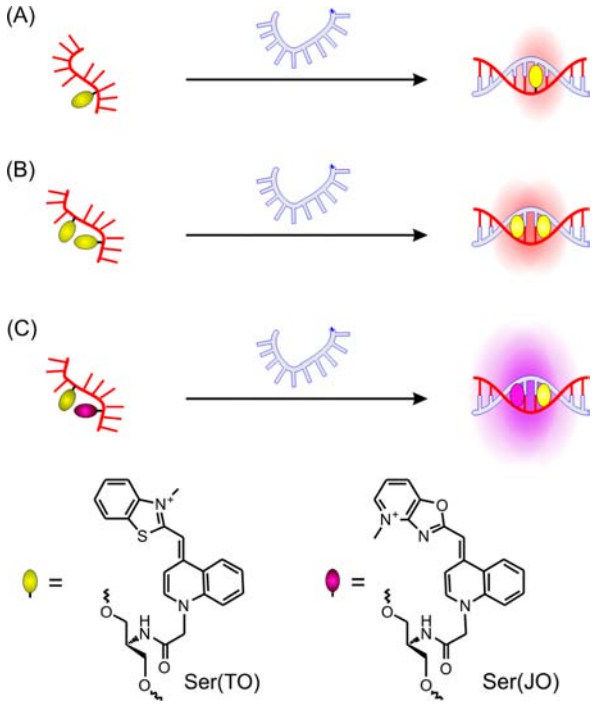

Figure 1. Schematic representation of (A) single TO, (B) double TO, and (C) TOJO-labeled DNA FIT-probes.

forces the dye to intercalate between predetermined base pairs.[35] The concomitant viscosity increase restricts torsions around the methine bridge and prolongs the lifetime of the TO excited state.[36] FIT-probes are highly responsive and exhibit marked increases in fluorescent emission upon hybridization.[31,37−42] However, the detection of RNA in autofluorescent tissue has remained challenging (vide infra). We sought a means to increase the brightness of fluorogenic DNA probes without compromising their responsiveness. To achieve this goal, we compared two approaches that involve the introduction of and energy transfer between two or more fluorescent base surrogates. We show that high brightness is obtained when two different, yet spectrally overlapping 'dye nucleobases' of the TO family are combined. The probes are brighter than fluorescein-based molecular beacons and conventional unquenched linear probes. The usefulness was demonstrated in imaging of RNA within a challenging tissue. Wash-free FISH with brightness enhanced DNA FIT-probes enabled the localization of *oskar* mRNA in developing ovaries of *Drosophila melanogaster* by using both narrow band and broad band excitation as applied in confocal fluorescence and cost-efficient wide-field epifluorescent microscopes, respectively.

RESULTS

Thiazole orange containing FIT-probes show remarkable responsiveness F_{ds}/F_{ss} of fluorescence upon hybridization.[37−41] However, the brightness of fluorescence F_{ds} in the probe bound state is limited by the extinction coefficient ($\varepsilon_{max} \approx$ 80000 L mol^{-1} cm^{-1}) and quantum yields ($\phi_{ds} \leq 0.35$). We envisaged two approaches to increase the brightness. In multi-TO-labeled probes, the incorporation of multiple 'TO bases' will allow for more effective absorption of photons (Figure 1B). The formation of the probe−target duplex will lead to an increase of TO emission which will be accompanied by a color change, owing to the separation of the TO units and the accompanying disruption of excitonic interactions. There is literature precedence for multilabeled hybridization probes, but their brightness has not been assessed.[25,43,44]

Alternatively, the 'TO base' will be accompanied by a second fluorescent base surrogate which shows a small bathochromic shift so that FRET could occur along an energy gradient (Figure 1C). This second dye should be selected to enable overlap of the absorption spectra, in which case the 'TO base' could act as a light collector. We chose the JO chromophore that is red-shifted by 10 nm.[45] Owing to a large extinction coefficient ($\varepsilon_{max} \approx$ 110 000 L mol^{-1} cm^{-1}) and a high quantum yield ($\phi_{max} \approx 0.8$), the JO dye is significantly brighter than TO, but the responsiveness of JO-based FIT-probes is low (vide infra). Nevertheless, for a combined TO/JO-containing FIT-probe we predicted a high responsiveness, because contact quenching will reduce the fluorescence of both dyes in single-stranded probes.

Synthesis. The TO and JO dyes were introduced into DNA by means of preformed nucleotide building blocks. Serinol-TO and serinol-JO phosphoramidites were synthesized by adapting a previously described method (Scheme S1).[34] Oligonucleotide synthesis was performed by applying known protocols.[46]

Dual-TO FIT-Probes. The incorporation of a second fluorescence base surrogate will change the optical properties of a FIT-probe. To rule out that the change of brightness is due to the sequence context around the second dye, we measured the dual label probes as well as both single label probes. The TO-nucleotide was walked through 15 positions of a 27mer oligonucleotide directed against a segment of *neuraminidase* mRNA of H1N1-influenza (Figure 2, left panel). The positional screen was used to characterize the optical properties as well as the effect of TO incorporation on duplex stability (Table S1). Particular emphasis was placed on the brightness (Br = ε(excitation) × quantum yield) of the probe−target complex.

The fluorescence quantum yields of single stranded TO-labeled probes were rather low (ϕ_{ss} = 0.02−0.04, see also Table S1). As previously reported, formation of the probe−target RNA-duplexes was accompanied by a significant enhancement of fluorescence quantum yields (up to ϕ_{ds} = 0.24, Figure 2A, see also Table S1).[34] Nine of the 15 probes tested provided useful (≥ 5-fold) enhancement of fluorescence intensity upon hybridization. However, the assessment of responsiveness was based on quantum yield enhancement and brightness values (1.7−9.3) rather than on fluorescence intensity, because this better complies with the experimental setup in fluorescence microscopic imaging, where emitted light is measured over wide band-pass filters.

In the single-stranded state, the dual TO-probes showed a rather low emission that was broad and red-shifted, from 515 nm (TO monomer emission) to up to 590 nm (Figure 2B, see also Figure S2). The absorbance spectra revealed a pronounced shoulder at 485 nm and in many cases the maximum was blue-shifted from 515 nm by 30 nm. These characteristics resemble the properties of the DNA stain TOTO and other TO dimers known to from H-aggregates.[25,47−49] Hybridization with the RNA target disrupted the TO-TO aggregates, resulting in

dx.doi.org/10.1021/ja410674h | J. Am. Chem. Soc. 2013, 135, 19025−19032

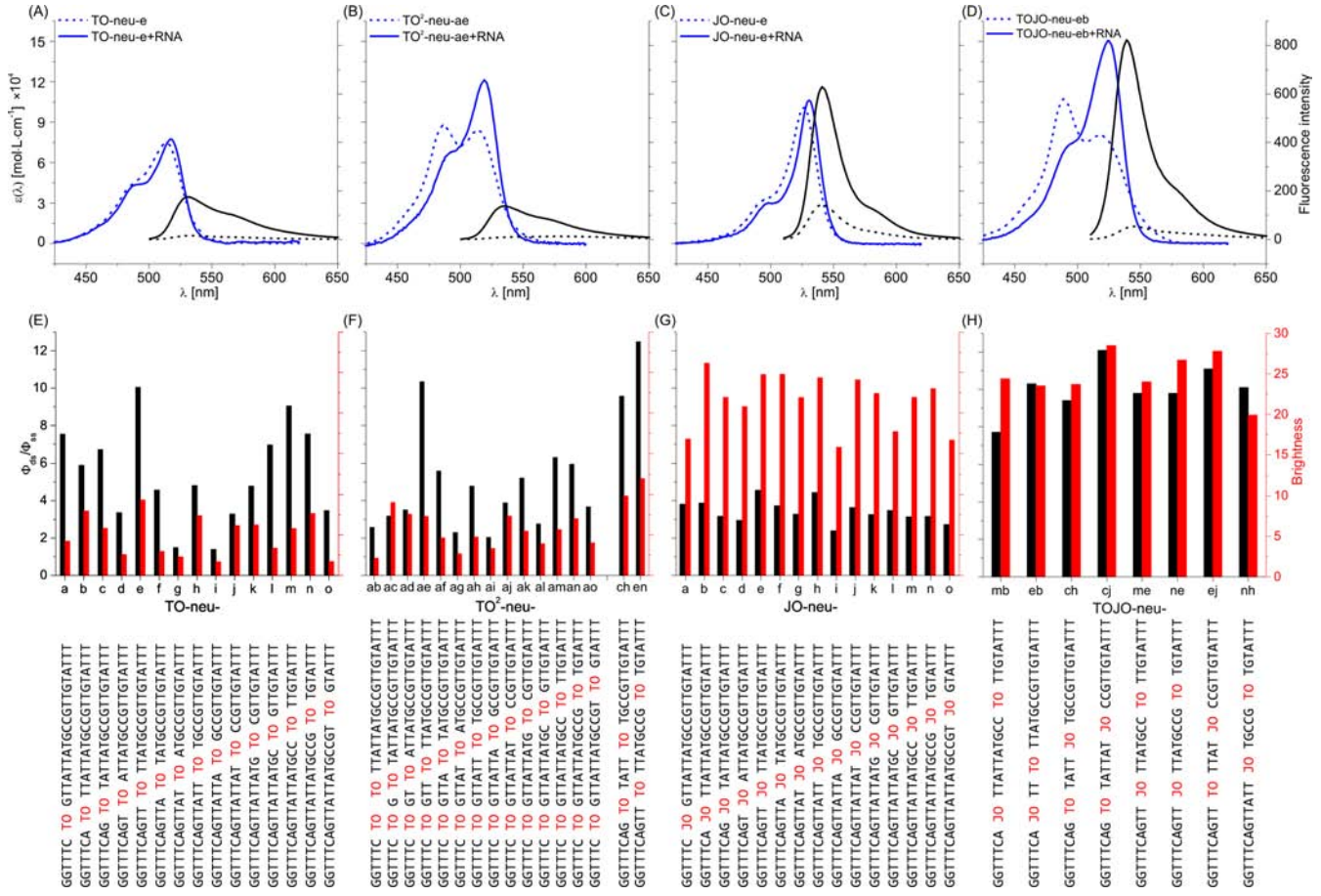

Figure 2. (A–D) Comparison of absorbance (blue) and fluorescence emission (black) of the indicated probes before (dashed) and after (solid) hybridization with complementary RNA (AAAUACAACGGC AUAAUAACUGAAACC). (E–H) Comparison of enhancement in fluorescence quantum yield (ϕ_{ds}/ϕ_{ss}, black bars) and brightness (red bars) in double-stranded state of single TO (E), double TO (F), single JO (G), and TO-JO-labeled probes (H). Conditions: 0.5 μM probe and 5 equiv RNA-target, when added, in PBS (100 mM NaCl, 10 mM Na_2HPO_4, pH 7) at 37 °C; for single and double TO: λ_{ex} = 485 nm, λ_{em} = 500–700 nm; for JO and TOJO: λ_{ex} = 500 nm, λ_{em} = 510–700 nm, $slit_{ex}$ = 5 nm, $slit_{em}$ = 5 nm. Scale bar are the same for (A-D) and (E-F).

absorbance and emission spectra of isolated TO dyes.[50] For multi-TO-labeled probes, the hybridization was accompanied by a change in emission color, which was observable even by the naked eye (Figure S4).

The introduction of a second TO nucleotide resulted in increased extinction coefficients. However, the quantum yields were reduced by nearly 50% and, therefore, brightness of the target-bound state did not improve (Figure 2B, see also Table S1). We characterized the distance dependence of this self-quenching effect (Figure 3, black diamonds). The local minima in self-quenching at 4 nt and 8 nt spacing probably reflect the orientation of the transition dipole moments.[51,52] Obviously, self-quenching was strongest when the TO units were in close proximity and generally lower at increased distance. Self-quenching is an effect of excitation energy homotransfer. The resulting delocalized excited states are believed to be particularly vulnerable to the quench processes.[53] Our experiments showed that the distance of 13 nucleotides was not sufficient to completely avoid self-quenching. Given the relatively small rise per base pair (2.9 Å) of an A-type DNA-RNA duplex, we assumed that rather long oligonucleotides would be required to disrupt homo-FRET between the TO dyes.[52,54]

The data exposed the significance of energy transfer between the TO-moieties in multilabeled probes. We surmised that the

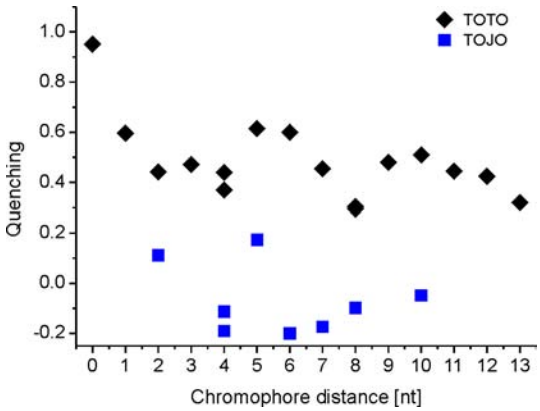

Figure 3. Distance dependency of quenching (Q) in dual-TO FIT probes (black diamonds) and TO/JO-labeled probes (blue square). $Q = 1 - F_{ds}(xy)/(F_{ds}(x) + F_{ds}(y))$ with $F_{ds}(xy)$ is the emission intensity at 535 nm of the double-labeled probe and $F_{ds}(x)$ or $F_{ds}(y)$ is the intensity of corresponding single labeled probes at 535 nm upon excitation at 485 nm.

TO unit with the lower quantum yield is limiting to the achievable overall quantum yield, that is, dissipation of energy would be predominantly caused by this 'weakest piece of the chain'. This assumption is in line with the optical properties of

dx.doi.org/10.1021/ja410674h | J. Am. Chem. Soc. 2013, 135, 19025–19032

Table 1. Comparison of TO-, JO-, and TO/JO-FIT-Probes with Molecular Beacon and Linear Probes[a]

probe	type	Sequence, X = TO, Y = JO	ϕ_{ss}	ϕ_{ds}	ϕ_{ds}/ϕ_{ss}	Br[b] [mL mol^{-1} cm^{-1}]
TO-neu-e	single TO	GGTTTCAGTT **X** TTATGCCGTTGTATTT	0.02	0.23	10.0	9.3
TO^2-neu-en	double TO	GGTTTCAGTT **X** TTATGCCG **X** TGTATTT	0.014	0.17	12.5	12.0
JO-neu-e	single JO	GGTTTCAGTT **Y** TTATGCCGTTGTATTT	0.14	0.63	4.6	18.9
TOJO-neu-cj	TOJO	GGTTTCAG **X** TATTAT **Y** CCGTTGTATTT	0.03	0.36	12.1	28.5
MB-neu-1	molecular beacon	6FAM-CCGACTTTCAGTTATTATGC CGTTGTATTTGTCGG-BHQ1	0.03[c]	0.26[c]	8.7	15.5[c]
FAM-neu	FISH	GGTTTCAGTTATTATGCCGTTGTATTT-6FAM	0.57	0.46	0.8	20.5

[a]Conditions: For TO see Figure 2; for JO and TO-JO see Figure 4. For MB-Neu-1 and FAM-Neu: 0.5 μM probe and 5 equiv RNA, when added, λ_{ex} = 485 nm, λ_{em} = 495−700 nm, in PBS at 37 °C, slit$_{ex}$ = 5 nm, slit$_{em}$ = 5 nm. [b]Brightness in target bound state. [c]Absorbance of the quencher was not subtracted.

probes that contain a third and a fourth TO-dye (Figure S3). Regardless of the number of TO units involved, the TO emission remained at similar intensity levels. Given the rather long reach of self-quenching by energy transfer we inferred that high brightness can only be obtained when 'weak pieces of the chain' are avoided. We constructed probes in which two strong emitters were positioned at distances with minimal self-quenching (4 or 8 nucleotides). The best dual-TO FIT-probe, **TO^2-neu-en**, showed an 18-fold enhancement of fluorescence intensity at 535 nm, as compared to 12-fold for the best single-TO FIT-probe, **TO-neu-n** (Table S1). However, the gain in brightness was only 29% (Figure 2D). We conclude that dual TO-labeling will not provide a notable advantage in RNA imaging experiments when emission is measured via the commonly used wide band-pass filters.

TO/JO-Labeled Probes. The experiments on dual-TO FIT-probes exposed self-quenching as the major factor limiting the achievable brightness. To improve upon brightness, we combined the responsive TO nucleotide with a highly emissive fluorophore such as the JO nucleotide. The JO dye was placed at 15 different positions within the 27 nt oligonucleotide (Figure 2C and G, see also Table S2 and Figure S5). The spectroscopic measurements confirmed that the JO-probes have higher absorbance and provide brighter emission than the corresponding TO-labeled probes (Figure 2E). The JO-labeled probes afforded high quantum yields, in both the single-stranded and the target-bound state. Thus, the fluorescence of single JO-probes is bright (Br = 13−20 mL mol^{-1} cm^{-1}) but shows comparably modest responsiveness ($\phi_{ds}/\phi_{ss} \approx 3-4$).

We next evaluated TO/JO-containing FIT-probes. Based on our findings with dual TO-labeled probes, we combined bright and responsive positions at various distances (2, 4, 5, 6, 7, 8, and 10 nt). The fluorescence spectroscopic measurements exposed remarkable performance of TO/JO-FIT-probes. The single-stranded TO/JO-probes were dark (Figure 2D and H; see also Figures S6 and S7). The quantum yields in absence of target remained nearly as low as for single TO-labeled probes (TO/JO-probes: ϕ_{ss} = 0.03−0.04) and significantly lower than the quantum yields of the corresponding JO-only probes (JO-probes: ϕ_{ss} = 0.14−0.16, Table S2). The shape and the change of the absorbance spectra upon hybridization suggest that the quenching of the JO emission is caused by contact quenching and/or exciplex formation (Figure 2D, see also Figures S6 and S7). The addition of RNA target led to remarkable florescence enhancements that exceeded the responsiveness of the best single TO-FIT-probes. Of note, 7 out of 8 probes provided an enhancement in quantum yield by factor ~10 upon duplex formation (Figure 2H). Most importantly, the quantum yields (ϕ_{ds} = 0.27−0.36) together with the high extinction coefficients, caused by spectral overlap, resulted in significantly improved brightness (Br = 20−29 mL mol^{-1} cm^{-1}).

To characterize distance effects in double-stranded TO/JO-labeled probes, the intensity of fluorescence at 535 nm was measured and compared with the sum of fluorescence intensities of the single labeled components. The quenching values $Q = 1 - F_{ds}(\mathrm{TOJO})/(F_{ds}(\mathrm{TO}) + F_{ds}(\mathrm{JO}))$ are considerably smaller than calculated for TO^2-probes and show rather small deviations from 0 (Figure 3, blue squares). Due to the high spectral overlap it is not possible to quantify energy transfer in TO/JO-probes by steady-state fluorescence measurements. However, in a 'gedankenexperiment' two scenarios may be distinguished: (1) At large distances and/or poor orientation of transition dipole moments energy transfer between TO and JO would be inefficient and the TO and JO emission signals would be additive. This would result in bright emission of the TO/JO-probe. (2) At shorter distance and/or suitable orientation of the chromophores energy transfer would become efficient. Following the gradient to longer wavelength, the energy transfer from TO to JO should be favored, because the spectral overlap between TO emission and JO absorption is higher than the overlap between JO emission and TO absorption (Figure S8). The TO dye would serve as a light collector and the brightness of emission would, again, be high due to the high extinction coefficient. This case may result in emission signals that exceed the sum of the components ($Q < 0$) because the relatively low TO quantum yield will no longer be limiting. Of note, six out of the eight TOJO-probes belonged to this category (see also Figure S9). Regardless of the mechanisms involved, we conclude that TO/JO probes combine the best of the TO and the JO worlds and allow for improvement of both probe responsiveness and the brightness.

Comparison of Different Fluorescent Probes. By using conventional fluorophore−quencher systems it is difficult to synergistically improve upon both responsiveness and brightness of fluorescent signaling. The FAM-labeled oligonucleotide **FAM-neu** (Table 1) may be regarded as the prototype of unquenched hybridization probes used in many applications including RNA fluorescent in situ hybridization (RNA FISH). These probes show high brightness of fluorescence (Br = 20.5 mL mol^{-1} cm^{-1}) but are virtually nonresponsive. This inevitably calls for carefully optimized wash protocols in order to remove unbound probe in imaging applications. The optimized FAM/quencher-labeled molecular beacon probe **MB-neu-1** provided a useful responsiveness, but, as expected, the presence of the quencher reduced the brightness in the target bound state by 25% compared to **FAM-neu**. The best single-TO FIT-probe **TO-neu-e** showed an even higher responsiveness, but the comparatively low brightness (Br =

dx.doi.org/10.1021/ja410674h | J. Am. Chem. Soc. 2013, 135, 19025−19032

9.3 mL mol^{-1} cm^{-1}) was of concern. By contrast, a high brightness was obtained for the JO containing FIT-probe **JO-neu-e**; however, its responsiveness was rather low. It was the combination of the TO and the JO nucleosides in **TOJO-neu-cj** that allowed for significant improvement of fluorescence signaling. This TOJO FIT-probe was even brighter than the conventional unquenched FAM-labeled probe **FAM-neu**.

Imaging *oskar* mRNA by Wash-Free Fluorescence in Situ Hybridization. We tested the FIT-probes within an intact tissue − the ovaries of *Drosophila melanogaster* − in situ. These organs are composed of egg-chambers at different developmental stages that consist of an oocyte connected to its 15 sibling nurse cells, encapsulated by a single layer of follicular epithelial cells (see Figure 4). As a target, we used the well-characterized *oskar* mRNA, which localizes at the posterior pole of oocytes from midoogenesis onward (see Figure 4).[55] We deliberately avoided detailed screening and examined 3 positions within the targeted segment (nt 2209−2229 of CDS) for JO and TO (Figure S10). The two best TO-positions were used for the construction of TO/JO FIT-probes (Table 2). The resulting **TOJO-osk-ac** and **TOJO-osk-ca** conferred very bright fluorescence signals upon hybridization. The JO labeled probes **JO-osk** were synthesized for comparison and showed the expected low responsiveness and high brightness (Br = 25−28 mL mol^{-1} cm^{-1}).

The brightest representative of each class (**TO-osk-a**, **JO-osk-a**, and **TOJO-osk-ca**, Figure S10) was evaluated in confocal fluorescence microscopy imaging experiments. We devised a simple and rapid protocol of performing fluorescent in situ hybridization (FISH). After a short fixation with 4% para-formaldehyde and a quick denaturation of RNA secondary structures by heat, the probes were applied to the dissected ovaries in presence of detergent (0.3% Tween-20) that permeabilizes the fixed cells and allows free diffusion of the probe into the cytoplasm. Following a 45 min long hybridization, the specimens were mounted on slides within the hybridization solution, without any washing steps. Due to the responsiveness of the DNA-FIT probes, *oskar* mRNA could be detected in oocytes of different developmental stages (Figure 4A-C, arrows) in patterns identical to those described previously, despite the presence of unbound probe molecules.[56] To assess the visual performance of the probes, we defined the signal-to-background ratio as the mean signal intensity at the posterior pole from stage 9 of oogenesis onward (Figure 4A-C, red arrows) over the mean signal measured in the surrounding follicular epithelium (Figure 4A, blue arrowheads), which does not express *oskar* mRNA. This ratio was found to be the greatest for the dual-labeled **TOJO-osk-ca**, both when excited at its maximum, 530 nm, or at 514 nm (Figure 4D).

As visual screening is usually carried out on cost-efficient instrumentation, such as on wide-field epifluorescent microscopes operated by a human observer, we decided to simulate this environment by using dual excitation to mimic a broadband excitation filter and a simple photomultiplier tube (PMT) with fully open pinhole and low gain on the detector side. We found that both egg-chamber morphology and *oskar* localization in the different developmental stages was, again, best visualized by the dual labeled **TOJO-osk-ca** probe (Figure 4A′). The use of **JO-osk-a** yielded a strong *oskar* signal; however, the elevated background both outside the egg-chamber and in the follicular epithelium reduced the contrast necessary to allow proper recognition of different features of the specimen (Figure 4B′). Conversely, in the case of the single TO labeled probes, the

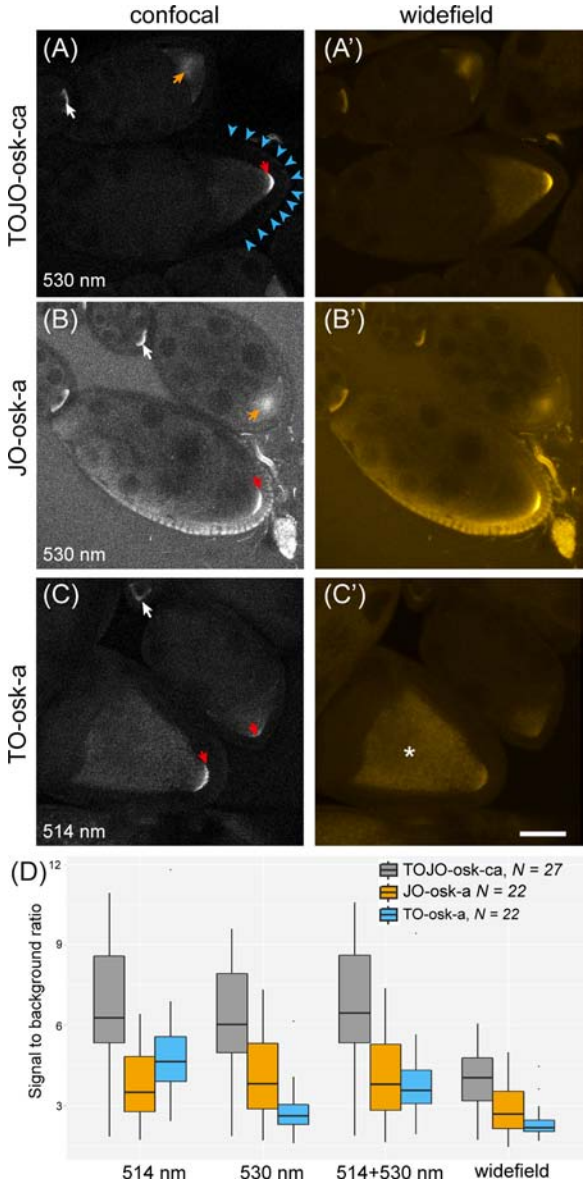

Figure 4. FIT probe signal in developing *Drosophila* oocytes. (A−C′) Representative images of FISH performed with 0.2 μM **TOJO-osk-ca** (A,A′), **JO-osk-a** (B,B′), or **TO-osk-a** (C,C′) probes. Confocal sections (A−C) were taken exciting the probes close to their maximal absorbance (indicated in the panels), widefield acquisition (A′−C′) was simulated by exciting with both 510−518 and 526−534 nm laser lines and imaging with open pinhole (7.7 Airy units). All images were adjusted to the same linear intensity scale. White arrows mark *oskar* mRNA in early oocytes. Orange arrows show central accumulation of mRNA during stage 8 of oogenesis. Red arrows tag stage 9−10, when *oskar* localizes to the posterior pole of the oocyte. The asterisk shows regions of strong autofluorescence by yolk granules within the oocytes (e.g., granular signal within the ooplasm in (C′). Bar is 50 μm. (D) Signal to background ratio (SBR) of FIT probes. Mean signal intensity was measured close to the posterior pole of stage 9−10 oocytes (red arrows) in an area engulfing accumulating *oskar* and was divided by the mean intensity measured within the surrounding follicle cells (indicated by blue arrowheads) using different excitation wavelengths and acquisition setup (514 nm, 530 nm, and 514 + 530 nm indicate confocal imaging; widefield indicates simulated widefield imaging as described above). (Mann−Whitney U test, $p < 0.001$, $\alpha = 0.05$). Number of oocytes (N) is indicated next to the key.

dx.doi.org/10.1021/ja410674h | J. Am. Chem. Soc. 2013, 135, 19025−19032

Table 2. TO-, JO-, and TO/JO-Probes Targeted against *oskar* RNA[a]

probe	Sequence, X = TO, Y = JO	T_M [°C]	ϕ_{ss}	ϕ_{ds}	ϕ_{ds}/ϕ_{ss}	Br[b] [mL mol^{-1} cm^{-1}]
TO-osk-a	CTCG **X** TTCA A TAAC T TGCAGT	56	0.04	0.31	8.7	14.3
TO-osk-b	CTCG T TTCA **X** TAAC T TGCAGT	55	0.07	0.18	2.7	8.3
TO-osk-c	CTCG T TTCA A TAAC **X** TGCAGT	55	0.02	0.16	7.5	6.4
TOJO-osk-ac	CTCG **X** TTCAATAAC **Y** TGCAGT	47	0.05	0.30	6.2	24.1
TOJO-osk-ca	CTCG **Y** TTCAATAAC **X** TGCAGT	51	0.06	0.42	7.6	29.1
JO-osk-a	CTCG **Y** TTCA A TAAC T TGCAGT	54	0.26	0.77	3.0	28.3
JO-osk-b	CTCG T TTCA **Y** TAAC T TGCAGT	56	0.53	0.79	1.5	26.1
JO-osk-c	CTCG T TTCA A TAAC **Y** TGCAGT	56	0.27	0.77	2.8	25.2

[a]Conditions: For TO-labeled probes see Figure 2; for JO and TOJO-labeled probes see Figure 4. [b]Brightness in target bound state.

reduced relative strength of the specific *oskar* signal caused a similar insufficiency of visibility (Figure 4C′).

Taken together, we have found that the DNA-FIT probes − especially the TO/JO labeled ones − are well-suited to perform rapid (∼1.5 h) FISH in complex tissues and allow sufficient visibility of the target even on non-cutting-edge equipment. Although conventional RNA probes which contain multiple DIG-labeled uracil nucleotides and multiple signal amplification steps, based on peroxidase-coupled anit-DIG antibodies, resulted in much brighter specimen with higher contrast (Figure S11), this standard technique of RNA visualization is very demanding of labor and reagents, rendering its use cumbersome and expensive in medium- and large-scale screens. The strongly reduced requirements of DNA-FIT probe based FISH for labor (∼1.5 h versus the ∼1.5 days for conventional FISH) and equipment while preserving sensitivity may turn this method a viable alternative in RNA localization screens of any scale.

DISCUSSION

The dynamic regulation of mRNA localization appears to be a widespread phenomenon that applies to a large fraction of exported transcripts.[57] Studying mRNA localization in the past two decades involved the extensive use of visual screening techniques,[57−59] which are generally very tedious, time-consuming applications and often are based on the localization of RNA binding proteins rather than the mRNA itself.[59] Fluorescent in situ hybridization is probably the most frequently used method for the detection and localization of specific RNA targets. However, the need for intensive washing and signal amplification is costly over time. It was our aim to explore whether FIT-probes with high responsiveness and brightness might enable rapid fluorescence microscopic analysis of cells and tissues by wash-free FISH. A variety of fluorescent oligonucleotide probes provide a turn-on of fluorescence upon hybridization. Recent contributions successfully applied in the analysis of intracellular targets include binary linear FRET probes[60] and various forms of DNA and PNA molecular beacons.[6,41,44,61,62] An exquisite responsiveness has been reported for improved molecular beacons.[8−31] However, most probes required the involvement of a nonfluorescent quencher, which limits the achievable brightness because quenching still occurs after the hairpin has been opened. The quencher has been omitted in wavelength-shifting beacons,[63] but remaining energy transfer in the target-bound state affects their responsiveness. In-stem beacons,[26−29] excimer-controlled beacons,[24] and, recently, multilabeled linear beacons[43] rely upon intimate contact between fluorescent base surrogates. Though remarkably responsive in vitro, the brightness of these multilabeled probes has not been assessed yet. One drawback that has to be considered when multiple base surrogates are incorporated within the target recognition sequence concerns the stability of the resulting probe−target complexes. It has been shown that the stability loss per base surrogate increases as the number of base replacements is increased.[43,64] In addition, our work on multi-TO-labeled probes suggests that the considerable extent of self-quenching limits the achievable brightness.

The work described herein shows that a combination of two different, yet spectrally overlapping, fluorophores can provide increases in brightness. The TO/JO FIT-probes contain two different fluorescent base surrogates. Torsional twisting around the methine bridges and intramolecular dye−dye interactions deplete the dyes excited states in the absence of target. Duplex formation hinders torsional twisting and contact-mediated energy transfer between the dyes. Additionally, the TO nucleoside can transfer energy to the JO emitter, as indicated by the broad excitation spectra (Figure S9). While JO itself is highly fluorescent, TO can serve as a light collector. This leads to very bright emission signals.

The TO/JO FIT-probes were brighter and showed higher enhancements in fluorescence quantum yield upon hybridization than sequence-analogous FAM/BHQ-labeled molecular beacons.[65] However, the environmental responsiveness of TO emission could be a reason for concern. The positional screening within a sequence directed against mRNA coding for neuraminidase of H1N1 influenza showed useful properties for > 50% of the tested probes. Two out of three positions evaluated for *oskar* FIT-probes proved to be useful. This resembles the efforts needed to optimize molecular beacons wherein the length and sequence of the stem structure must be adjusted to prevent undesired opening and, yet, permit high signal gain upon hybridization with the target (Figure S12).

The brightness and the mechanism of fluorescence signaling by TO/JO−DNA FIT-probes is different from other thiazole orange-containing probes. The so-called Light-Up probes contain a TO dye appended to one of the terminal ends of PNA.[66] Their brightness is limited due to the use of a single TO unit. In the ECHO probes, TO dimers connect via a long linkage to sequence-internal nucleobases.[67] The TO dyes form an H-aggregate in the single strand that is disrupted upon hybridization and the accompanying intercalation. ECHO probes optimized for avoidance of intra- and intermolecule dimerization show high responsiveness which enabled the detection of abundant targets by RNA-FISH.[68,69] While brightness has not been characterized, published data suggests that the brightness of the TO-dimer-labeled ECHO-probes is comparable to analogous probes containing a single TO dye.[49,70] A recent report described RNA duplexes in which one strand contained a TO-unit, while the other strand featured a

thiazole red or Cy3 unit.[71] Energy transfer between the two dyes was used to follow the integrity of the RNA duplex in a cellular context. The signaling intensity measured after occurrence of the biological event is, again, limited by the emission of a single TO-like dye.

The design criteria for bright and responsive hybridization probes that we have described involve the use of a dye pair that (a) senses local changes of the structure, (b) enables contact-mediated quenching in the single-stranded state, (c) provides overlapping absorption spectra, and (d) includes a bright acceptor that enables efficient FRET after probe hybridization. In support of this guideline, many criteria have been met in TO/ICC-containing PNA FIT-probes, which have been reported to provide bright fluorescence upon hybridization.[31] However, the terminally appended ICC dye does not have the ability to sense structural changes in the environment. This probably explains why TO/JO−DNA FIT-probes afford a higher responsiveness than sequence analogous TO/ICC-PNA FIT-probes (Figure S13).

One could surmise that the introduction of two JO dyes could also lead to bright and responsive probes. Though the dual JO-probes may show a higher responsiveness than single JO-probes, we expect little increase of brightness, due to self-quenching.

CONCLUSION

We have developed fluorescence turn-on hybridization probes that combine high responsiveness of fluorescence with a high brightness of the measured emission signal. Such properties are required in wash-free FISH and live cell RNA imaging, when unbound probes cannot be washed away and the target must be detected above the relatively high autofluorescent background of cells or tissues. We demonstrated that this goal cannot be achieved by simply increasing the number of thiazole orange fluorophores per probe molecule. The experiments on dual-TO FIT-probes exposed self-quenching as the major factor limiting the achievable brightness, and the long reach of homo-FRET would require the synthesis of very long hybridization probes. Rather, we showed that significant enhancements of brightness and responsiveness can be achieved when two different, yet spectrally overlapping, fluorescent base surrogates (TO and JO) are combined. Contact quenching and the absence of intercalation opportunities render single-stranded TO/JO FIT-probes dark. These paths for depletion of excited states are blocked in the probe−target duplex. The overlap between TO and JO absorption spectra and FRET leads to very bright JO emission (calculated brightness at λ_{ex}(max) = 516 nm up to 43 mL mol^{-1} cm^{-1}).

We have developed a protocol to analyze the localization of *oskar* mRNA in dissected ovaries from *Drosophila melanogaster* by means of fluorescence microscopic imaging. Our experiments revealed that the TO/JO FIT-probes are well suited to perform rapid (~1.5 h) FISH in complex tissues. An image analysis exposed the usefulness of the TO/JO FIT-probes which provided for significantly higher signal-to-background ratios than TO-only and JO-only hybridization probes at various wavelengths (485, 514, 530 nm were tested), and we demonstrated that this feature enables RNA imaging under (simulated) wide-field excitation conditions. We expect that the TO/JO FIT-probes should prove useful in other RNA imaging endeavors including RNA imaging in live cells.

ASSOCIATED CONTENT

Supporting Information

Experimental and characterization data, NMR spectra of compounds, fluorescence and absorbance spectra of probes. This material is available free of charge via the Internet at http://pubs.acs.org.

AUTHOR INFORMATION

Corresponding Author

*E-mail: oliver.seitz@chemie.hu-berlin.de

Notes

The authors declare no competing financial interest.

ACKNOWLEDGMENTS

This work was financially supported by the Deutsche Forschungsgemeinschaft and by a Kekulé-fellowship of Fonds der Chemischen Industrie for Felix Hövelmann, and by an EMBL Interdisciplinary Postdoctoral Fellowship (EIPOD) to Imre Gaspar.

REFERENCES

(1) Santangelo, P. J.; Nitin, N.; Bao, G. *J. Biomed. Opt.* **2005**, *10*, 44025.
(2) St Amand, A. L.; Frank, D. N.; De Groote, M. A.; Pace, N. R. *J. Clin. Microbiol.* **2005**, *43*, 1505.
(3) Tyagi, S. *Nat. Methods* **2009**, *6*, 331.
(4) Armitage, B. A. *Curr. Opin. Chem. Biol.* **2011**, *15*, 806.
(5) Mackay, I. M.; Arden, K. E.; Nitsche, A. *Nucleic Acids Res.* **2002**, *30*, 1292.
(6) Bao, G.; Rhee, W. J.; Tsourkas, A. *Annu. Rev. Biomed. Eng.* **2009**, *11*, 25.
(7) Tyagi, S.; Kramer, F. R. *Nat. Biotechnol.* **1996**, *14*, 303.
(8) Lin, Y. W.; Ho, H. T.; Huang, C. C.; Chang, H. T. *Nucleic Acids Res.* **2008**, *36*, e123.
(9) Lin, Y. H.; Tseng, W. L. *Chem. Commun.* **2012**, *48*, 6262.
(10) Wang, L.; Yang, C. Y. J.; Medley, C. D.; Benner, S. A.; Tan, W. H. *J. Am. Chem. Soc.* **2005**, *127*, 15664.
(11) Bourdoncle, A.; Torres, A. E.; Gosse, C.; Lacroix, L.; Vekhoff, P.; Le Saux, T.; Jullien, L.; Mergny, J. L. *J. Am. Chem. Soc.* **2006**, *128*, 11094.
(12) Grossmann, T. N.; Roglin, L.; Seitz, O. *Angew. Chem., Int. Ed.* **2007**, *46*, 5223.
(13) Yang, C. J.; Wang, L.; Wu, Y. R.; Kim, Y. M.; Medley, C. D.; Lin, H.; Tan, W. H. *Nucleic Acids Res.* **2007**, *35*, 4030.
(14) Johansson, M. K.; Cook, R. M. *Chem.—Eur. J.* **2003**, *9*, 3466.
(15) Kang, W. J.; Cho, Y. L.; Chae, J. R.; Lee, J. D.; Choi, K. J.; Kim, S. *Biomaterials* **2011**, *32*, 1915.
(16) Dubertret, B.; Calame, M.; Libchaber, A. J. *Nat. Biotechnol.* **2001**, *19*, 365.
(17) Yeh, H. Y.; Yates, M. V.; Mulchandani, A.; Chen, W. *Chem. Commun.* **2010**, *46*, 3914.
(18) Jayagopal, A.; Halfpenny, K. C.; Perez, J. W.; Wright, D. W. *J. Am. Chem. Soc.* **2010**, *132*, 9789.
(19) Yeh, H. C.; Sharma, J.; Shih, I. M.; Vu, D. M.; Martinez, J. S.; Werner, J. H. *J. Am. Chem. Soc.* **2012**, *134*, 11550.
(20) Li, F.; Huang, Y.; Yang, Q.; Zhong, Z. T.; Li, D.; Wang, L. H.; Song, S. P.; Fan, C. H. *Nanoscale* **2010**, *2*, 1021.
(21) Lu, C. H.; Li, J.; Liu, J. J.; Yang, H. H.; Chen, X.; Chen, G. N. *Chem.—Eur. J.* **2010**, *16*, 4889.
(22) Huang, P. J. J.; Liu, J. W. *Anal. Chem.* **2012**, *84*, 4192.
(23) He, S.; Song, B.; Li, D.; Zhu, C.; Qi, W.; Wen, Y.; Wang, L.; Song, S.; Fang, H.; Fan, C. *Adv. Funct. Mater.* **2010**, *20*, 453.
(24) Haner, R.; Biner, S. M.; Langenegger, S. M.; Meng, T.; Malinovskii, V. L. *Angew. Chem., Int. Ed.* **2010**, *49*, 1227.
(25) Berndl, S.; Wagenknecht, H.-A. *Angew. Chem., Int. Ed.* **2009**, *48*, 2418.

(26) Kashida, H.; Takatsu, T.; Fujii, T.; Sekiguchi, K.; Liang, X. G.; Niwa, K.; Takase, T.; Yoshida, Y.; Asanuma, H. *Angew. Chem., Int. Ed.* **2009**, *48*, 7044.
(27) Hara, Y.; Fujii, T.; Kashida, H.; Sekiguchi, K.; Liang, X. G.; Niwa, K.; Takase, T.; Yoshida, Y.; Asanuma, H. *Angew. Chem., Int. Ed.* **2010**, *49*, 5502.
(28) Holzhauser, C.; Wagenknecht, H.-A. *Angew. Chem., Int. Ed.* **2011**, *50*, 7268.
(29) Asanuma, H.; Osawa, T.; Kashida, H.; Fujii, T.; Liang, X. G.; Niwa, K.; Yoshida, Y.; Shimadad, N.; Maruyama, A. *Chem. Commun.* **2012**, *48*, 1760.
(30) Socher, E.; Bethge, L.; Knoll, A.; Jungnick, N.; Herrmann, A.; Seitz, O. *Angew. Chem., Int. Ed.* **2008**, *47*, 9555.
(31) Socher, E.; Knoll, A.; Seitz, O. *Org. Biomol. Chem.* **2012**, *10*, 7363.
(32) Silverman, A. P.; Kool, E. T. *Trends Biotechnol.* **2005**, *23*, 225.
(33) Gorska, K.; Keklikoglou, I.; Tschulena, U.; Winssinger, N. *Chem. Sci.* **2011**, *2*, 1969.
(34) Hovelmann, F.; Bethge, L.; Seitz, O. *ChemBioChem* **2012**, *13*, 2072.
(35) Bethge, L.; Singh, I.; Seitz, O. *Org. Biomol. Chem.* **2010**, *8*, 2439.
(36) Karunakaran, V.; Perez Lustres, J. L.; Zhao, L.; Ernsting, N. P.; Seitz, O. *J. Am. Chem. Soc.* **2006**, *128*, 2954.
(37) Kohler, O.; Venkatrao, D.; Jarikote, D. V.; Seitz, O. *ChemBioChem* **2005**, *6*, 69.
(38) Jarikote, D. V.; Krebs, N.; Tannert, S.; Roder, B.; Seitz, O. *Chem.—Eur. J.* **2007**, *13*, 300.
(39) Socher, E.; Jarikote, D. V.; Knoll, A.; Roglin, L.; Burmeister, J.; Seitz, O. *Anal. Biochem.* **2008**, *375*, 318.
(40) Kummer, S.; Knoll, A.; Socher, E.; Bethge, L.; Herrmann, A.; Seitz, O. *Angew. Chem., Int. Ed. Engl.* **2011**, *50*, 1931.
(41) Kummer, S.; Knoll, A.; Sucher, E.; Bethge, L.; Herrmann, A.; Seitz, O. *Bioconjugate Chem.* **2012**, *23*, 2051.
(42) Torres, A. G.; Fabani, M. M.; Vigorito, E.; Williams, D.; Al-Obaidi, N.; Wojciechowski, F.; Hudson, R. H.; Seitz, O.; Gait, M. J. *Nucleic Acids Res.* **2012**, *40*, 2152.
(43) Asanuma, H.; Akahane, M.; Kondo, N.; Osawa, T.; Kato, T.; Kashida, H. *Chem. Sci.* **2012**, *3*, 3165.
(44) Kubota, T.; Ikeda, S.; Okamoto, A. *Bull. Chem. Soc. Jpn.* **2009**, *82*, 110.
(45) Bethge, L.; Jarikote, D. V.; Seitz, O. *Bioorg. Med. Chem.* **2008**, *16*, 114.
(46) Caruthers, M. H.; Barone, A. D.; Beaucage, S. L.; Dodds, D. R.; Fisher, E. F.; McBride, L. J.; Matteucci, M.; Stabinsky, Z.; Tang, J. Y. *Methods Enzymol.* **1987**, *154*, 287.
(47) Rye, H. S.; Yue, S.; Wemmer, D. E.; Quesada, M. A.; Haugland, R. P.; Mathies, R. A.; Glazer, A. N. *Nucleic Acids Res.* **1992**, *20*, 2803.
(48) Ikeda, S.; Kubota, T.; Yuki, M.; Okamoto, A. *Angew. Chem., Int. Ed.* **2009**, *48*, 6480.
(49) Ikeda, S.; Okamoto, A. *Chem. Asian J.* **2008**, *3*, 958.
(50) Only side-by-side positioned TO-nucleotides (0 nt distance) remained aggregated (Figure S2).
(51) Kato, T.; Kashida, H.; Kishida, H.; Yada, H.; Okamoto, H.; Asanuma, H. *J. Am. Chem. Soc.* **2013**, *135*, 741.
(52) Borjesson, K.; Preus, S.; El-Sagheer, A. H.; Brown, T.; Albinsson, B.; Wilhelmsson, L. M. *J. Am. Chem. Soc.* **2009**, *131*, 4288.
(53) Teo, Y. N.; Wilson, J. N.; Kool, E. T. *Chem.—Eur. J.* **2009**, *15*, 11551.
(54) Robertson, K. L.; Yu, L. P.; Armitage, B. A.; Lopez, A. J.; Peteanu, L. A. *Biochemistry* **2006**, *45*, 6066.
(55) Bratu, D. P.; Cha, B. J.; Mhlanga, M. M.; Kramer, F. R.; Tyagi, S. *Proc. Natl. Acad. Sci. U. S. A.* **2003**, *100*, 13308.
(56) Ghosh, S.; Marchand, V.; Gaspar, I.; Ephrussi, A. *Nat. Struct. Mol. Biol.* **2012**, *19*, 441.
(57) Lecuyer, E.; Yoshida, H.; Parthasarathy, N.; Alm, C.; Babak, T.; Cerovina, T.; Hughes, T. R.; Tomancak, P.; Krause, H. M. *Cell* **2007**, *131*, 174.
(58) Wilson, J. E.; Connell, J. E.; Schlenker, J. D.; Macdonald, P. M. *Dev. Genet.* **1996**, *19*, 199.
(59) Martin, S. G.; Leclerc, V.; Smith-Litiere, K.; St Johnston, D. *Development* **2003**, *130*, 4201.
(60) Tsuji, A.; Koshimoto, H.; Sato, Y.; Hirano, M.; Sei-Iida, Y.; Kondo, S.; Ishibashi, K. *Biophys. J.* **2000**, *78*, 3260.
(61) Kam, Y.; Rubinstein, A.; Nissan, A.; Halle, D.; Yavin, E. *Mol. Pharm.* **2012**, *9*, 685.
(62) Holzhauser, C.; Berndl, S.; Menacher, F.; Breunig, M.; Gopferich, A.; Wagenknecht, H. A. *Eur. J. Org. Chem.* **2010**, 1239.
(63) Santangelo, P. J.; Nix, B.; Tsourkas, A.; Bao, G. *Nucleic Acids Res.* **2004**, *32*, e57.
(64) Randolph, J. B.; Waggoner, A. S. *Nucleic Acids Res.* **1997**, *25*, 2923.
(65) Johansson, M. K.; Fidder, H.; Dick, D.; Cook, R. M. *J. Am. Chem. Soc.* **2002**, *124*, 6950.
(66) Svanvik, N.; Westman, G.; Wang, D. Y.; Kubista, M. *Anal. Biochem.* **2000**, *281*, 26.
(67) Ikeda, S.; Kubota, T.; Kino, K.; Okamoto, A. *Bioconjugate Chem.* **2008**, *19*, 1719.
(68) Ikeda, S.; Kubota, T.; Yuki, M.; Yanagisawa, H.; Tsuruma, S.; Okamoto, A. *Org. Biomol. Chem.* **2010**, *8*, 546.
(69) Wang, D. O.; Matsuno, H.; Ikeda, S.; Nakamura, A.; Yanagisawa, H.; Hayashi, Y.; Okamoto, A. *RNA* **2012**, *18*, 166.
(70) Wang, D. O.; Okamoto, A. *J. Photochem. Photobiol., C* **2012**, *13*, 112.
(71) Kamiya, Y.; Ito, A.; Ito, H.; Urushihara, M.; Takai, J.; Fujii, T.; Liang, X.; Kashida, H.; Asanuma, H. *Chem. Sci.* **2013**, *4*, 4016.